Available online at www.sciencedirect.com
SCIENCE DIRECT®
International Journal of Heat and Mass Transfer 47 (2004) 4685–4695
International Journal of HEAT and MASS TRANSFER
www.elsevier.com/locate/ijhmt

# Green's function solution of temperature field for flow in porous passages

A. Haji-Sheikh [a,*], W.J. Minkowycz [b], E.M. Sparrow [c]

[a] Department of Mechanical and Aerospace Engineering, The University of Texas at Arlington, 500 West First Street, Arlington, TX 76019-0023, USA
[b] Department of Mechanical and Industrial Engineering, University of Illinois at Chicago, Chicago, IL 60607-7022, USA
[c] Department of Mechanical Engineering, University of Minnesota, Minneapolis, MN 55455-0111, USA

Received 29 April 2004; received in revised form 1 June 2004
Available online 20 July 2004

**Abstract**

Recently, the heat transfer in porous passages has received attention from many investigators. The Green's function solution method can serve as a powerful tool to accomplish this task of providing solutions to this type of problems with or without the effect of axial conduction. The study of heat transfer with emphasis on frictional heating, in the absence of axial conduction, is the subject of this presentation. As a simple example, consideration is given to the numerical study of the heat transfer in flow between two impermeable parallel plates. The individual effects of temperature change at the walls, frictional heating, and the combined effects are examined. The data shows that the combined effects can produce removable singularities under certain boundary conditions. To avoid the occurrence of singularities in these types of applications, certain heat transfer parameters are presented in different but basic forms.


*Keywords:* Green's function; Porous passages; Frictional heating; Channel flow; Convection

## 1. Introduction

The Green's function solution is a powerful tool to accommodate linear heat transfer problems in the presence of volumetric heat source and various types of boundary conditions. Such a solution provides insight into the general problem of flow in porous passages with impermeable walls. For simplicity of this presentation, the axial conduction is ignored. The study of the effects of axial conduction is deferred since it requires an extensive modification of functional relations beyond the scope of this presentation.

A number of recent studies use a general flow model known as the Brinkman–Forschheimer–extended Darcy model. Kaviany [1] used the Brinkman–extended Darcy model to numerically obtain solution of laminar flow in a porous channel bounded by isothermal parallel plates. Study of flow in porous media is reported in various textbooks, e.g., in Nield and Bejan [2], Kaviany [3], and Vafai [4]. Angirasa [5] discusses the history of development of transport equations in porous media and finite difference simulations.

This study reports the exact mathematical relations for heat transfer computation using the Green's function solution [6] in the entrance region for ducts with different cross-sections. The entrance flow problems in the presence of frictional heating and axial conduction are reported in [7] for parallel plate channels and in [8] for circular pipes. A discussion as to the form of the frictional heating term is in [9] and a modification is recommended in [10].

In this study the heat transfer in the presence of frictional heating in parallel plate channels are analyzed

* Corresponding author. Tel.: +1-817-272-2010; fax: +1-817-272-2952.
*E-mail address:* haji@mae.uta.edu (A. Haji-Sheikh).

0017-9310/$ - see front matter © 2004 Elsevier Ltd. All rights reserved.
doi:10.1016/j.ijheatmasstransfer.2004.06.008

**Nomenclature**

| | |
|---|---|
| $A$ | area, $m^2$ |
| $A_m$, $a_i$ | coefficients |
| $B_m$ | coefficient |
| $Br$ | Brinkman number, $Br = \mu U^2 H^2/[Kk_e(T_1 - T_2)]$ |
| $C$ | capacitance, $\rho c_p$ |
| $c_n$ | coefficients |
| $c_p$ | specific heat, J/kg K |
| $Da$ | Darcy number, $K/H^2$ |
| $D_h$ | hydraulic diameter, m |
| $d_n$ | coefficients |
| $Ec$ | Eckert number, $U^2/[c_p(T_1 - T_2)]$ |
| $F_s$ | source function |
| $h$ | heat transfer coefficient, $W/m^2$ K |
| $\bar{h}$ | average heat transfer coefficient, $W/m^2$ K |
| $H$ | channel dimension, see Fig. 3 |
| $i$,$j$ | indices |
| $K$ | permeability, $m^2$ |
| $k_e$ | effective thermal conductivity |
| $M$ | $\mu_e/\mu$ |
| $Nu_H$ | Nusselt number, $hH/k_e$ |
| $m$,$n$ | indices |
| $Pe$ | Peclet number, $\rho c_p L_c U/k_e$ |
| $Pr$ | Prandtl number, $\mu_e c_p/k_e$ |
| $p$ | pressure, Pa |
| $q_w$ | wall heat flux, $W/m^2$ |
| $\bar{q}_w$ | average wall heat flux, $W/m^2$ |
| $S$ | volumetric heat source, $W/m^3$ |
| $T$ | temperature, K |
| $T_i$ | temperature at $x = 0$, K |
| $T_w$ | wall temperature, K |
| $u$ | velocity, m/s |
| $\bar{u}$ | $\bar{u} = \mu u/(\Phi H^2)$ |
| $U$ | average velocity, m/s |
| $\overline{U}$ | average value of $\bar{u}$ |
| $x$ | axial coordinate, m |
| $\bar{x}$ | $x/(PeH)$ |
| $y$,$z$ | coordinates, m |
| $Y$ | eigenfunction |

*Greek symbols*

| | |
|---|---|
| $\Theta$ | $(T - T_w/T_i - T_w)$ |
| $\lambda_m$ | eigenvalues |
| $\mu$ | fluid viscosity, N s/$m^2$ |
| $\mu_e$ | effective viscosity, N s/$m^2$ |
| $\rho$ | density, $kg/m^3$ |
| $\Phi$ | $-\partial p/\partial x$ |
| $\psi$ | coefficient, Eq. (19b) |
| $\omega$ | $1/\sqrt{MDa}$ |

*Subscripts*

| | |
|---|---|
| b | bulk |
| I | entrance effects |
| S | heat source effects |
| W | wall effects |

using a Green's function solution. This is an exact series solution that requires the computation of a set of eigenvalues. This presentation includes a discussion of convergence and accuracy of the solution when using a finite number of eigenvalues. The combined effect of the frictional heating and the wall temperature change shows the existence of certain singularities.

## 2. General formulation of velocity field

The computation of heat transfer rates to a fully developed flow through a porous media confined within a duct with constant cross-section, Fig. 1, requires knowledge of the velocity profile. It is assumed that the thermophysical properties remain constant and the Brinkman momentum equation holds for fully developed flow,

$$\mu_e\left(\frac{\partial^2 u}{\partial y^2} + \frac{\partial^2 u}{\partial z^2}\right) - \frac{\mu}{K}u - \frac{\partial p}{\partial x} = 0 \tag{1}$$

When the pressure gradient $\Phi = -\partial p/\partial x$ is a constant, one can use the effective viscosity $\mu_e$, the fluid viscosity $\mu$, the permeability $K$, and a characteristic length $L_c$ in order to set Eq. (1) in dimensionless form,

$$M\left(\frac{\partial^2 \bar{u}}{\partial \bar{y}^2} + \frac{\partial^2 \bar{u}}{\partial \bar{z}^2}\right) - \frac{1}{Da}\bar{u} - 1 = 0 \tag{2}$$

The dimensionless parameters are $\bar{y} = y/L_c$, $\bar{z} = z/L_c$, $M = \mu_e/\mu$, $\bar{u} = \mu u/(\Phi L_c^2)$, and $Da = K/L_c^2$ is the Darcy number. The solution of Eq. (2), with the boundary condition $\bar{u} = 0$ at the wall, is often obtainable analytically. Once the velocity is determined, the relation

$$U = \frac{1}{A}\int_A u\,\mathrm{d}y \tag{3}$$

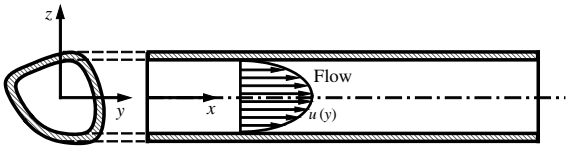


Fig. 1. Schematic of a passage filled with porous materials.

provides the mean velocity. Since fluid flows in the direction of $x$, the Laplace operator in Eq. (2) takes different forms depending on the coordinate system.

## 3. General formulation of temperature field

Assuming the condition of local thermal equilibrium to be valid, the energy equation when the velocity is fully developed and thermophysical properties are independent of temperature is

$$Cu\frac{\partial T}{\partial x}=\frac{\partial}{\partial x}\left(k_e\frac{\partial T}{\partial x}\right)+\frac{\partial}{\partial y}\left(k_e\frac{\partial T}{\partial y}\right)+\frac{\partial}{\partial z}\left(k_e\frac{\partial T}{\partial z}\right)-mT+S(x,y,z) \tag{4}$$

Here, $S(x,y,z)$ is the classical volumetric heat source that includes the contribution of frictional heating in various forms. The parameters $C$ and $k_e$ are the equivalent thermal capacitance and the thermal conductivity, respectively. Mathematically, it is possible to hypothesize that $C=C(y,z)$ and $k_e=k_e(y,z)$; however, they remain independent of $x$ in subsequent analysis. Using these specified conditions and for convenience of mathematical formulations, Eq. (4) becomes

$$\frac{\partial}{\partial y}\left(k_e\frac{\partial T}{\partial y}\right)+\frac{\partial}{\partial z}\left(k_e\frac{\partial T}{\partial z}\right)-m^2T+S(x,y,z)=Cu\frac{\partial T}{\partial x}-k_e\frac{\partial^2 T}{\partial x^2} \tag{5}$$

In the following formulations, as a shorthand notation, the first two terms on the left side of Eq. (5) will be designated as $\nabla\cdot(k_e\nabla T)$. The second term on the right side of Eq. (5) describes the contribution of axial heat conduction. The emphasis of this presentation is the study of the effect of frictional heating in passages filed with porous materials. For this reason and to simplify the mathematical procedures, consideration is given to flow with a large Peclet number; hence the effect of axial conduction is not included in the subsequent formulations.

## 4. Formulation of the Green's function solution equation

It is preferable to present the derivation of the Green's function solution using the basic variables in their most general form. However, in mathematical formulations, the following assumptions apply:

1. There is a local thermal equilibrium condition throughout the fully saturated medium.
2. The flow is fully developed and therefore $u=(u,y,z)$.
3. There is no work due to compression because of condition 2.
4. The thermophysical properties are independent of the axial coordinate.
5. The steady state condition exists throughout the medium.
6. The effect of axial heat conduction is negligible (large Peclet number).

The Green's function mathematically describes the contribution of the source $C\delta(\mathbf{r}-\mathbf{r}')\delta(x-\xi)$. The parameter $\mathbf{r}$ stands for $(y,z)$ and $\mathbf{r}'$ stands for $(y',z')$. The Green's function $G=G(r,x|r',\xi)$ indicates the effect of a source located at $(y',z')$ and at axial location $\xi$ detectable at $(y,z)$ within a cross-section that is located at the axial coordinate $x$. A differential equation that describes the Green's function is

$$\nabla\cdot(k_e\nabla G)-m^2G+C\delta(\mathbf{r}-\mathbf{r}')\delta(x-\xi)=Cu\frac{\partial G}{\partial x} \tag{6}$$

The Green's function $G$ satisfies homogeneous boundary conditions along the boundary (contour) of the passage and the conditions $G=0$ at $x=0$. The next task is to find a generalized Green's function solution to this parabolic form of the energy equation. Changing the derivatives in Eq. (6) with respect to $y$ and $z$ to those with respect to $y'$ and $z'$ and derivatives with respect to $x$ to those with respect to $-\xi$ provides the following relation.

$$\nabla_o\cdot(k_e\nabla_o G)-m^2G+C\delta(\mathbf{r}-\mathbf{r}')\delta(x-\xi)=-Cu\frac{\partial G}{\partial \xi} \tag{7}$$

where $\nabla_o$ implies that the grad operator is in $\mathbf{r}'$ or $(y',z')$ space. Also, Eq. (5) is written in $\mathbf{r}'$ space and when $x$ is replaced by $\xi$ as

$$\nabla_o\cdot(k_e\nabla_o T)-m^2T+S(\mathbf{r}',\xi)=Cu\frac{\partial T}{\partial \xi} \tag{8}$$

Multiplying Eq. (7) by $T$ and Eq. (8) by $G$, then subtracting the results produces the relation

$$G\nabla_o\cdot(k_e\nabla_o T)-T\nabla_o\cdot(k_e\nabla_o G)+GS(\mathbf{r}',\xi)-C\delta(\mathbf{r}-\mathbf{r}')\delta(x-\xi)T=Cu\frac{\partial(TG)}{\partial\xi} \tag{9}$$

Using the standard procedure described in Beck et al. [6], both sides of Eq. (9) are to be integrated over the cross-section area $A$ in $\mathbf{r}'$ space and over $\xi$ from 0 to $x+\varepsilon$ where $\varepsilon$ is a small positive number. Following application of the Green's theorem and after letting $\varepsilon$ to go to zero, the result is

$$T(r,t)=\frac{1}{C(\mathbf{r})}\left\{\int_{\xi=0}^{x}d\xi\int_{\Gamma}k_e(\mathbf{r})\left(G\frac{\partial T}{\partial n}-T\frac{\partial G}{\partial n}\right)_{\Gamma'}d\Gamma'+\int_{\xi=0}^{x}d\xi\int_{A}GS(\mathbf{r}',\xi)\,dA'+\int_{A}C(\mathbf{r})u(\mathbf{r})G(\mathbf{r},x|r',0)T(\mathbf{r}',0)\,dA'\right\} \tag{10}$$

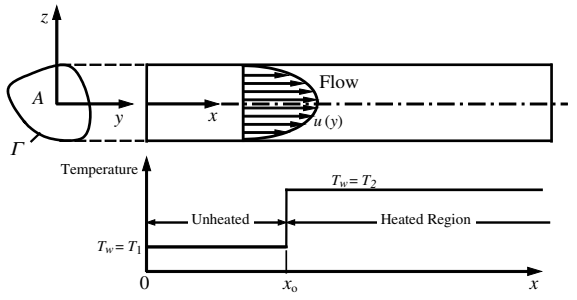


Fig. 2. Illustration of expected boundary condition of a passage filled with porous materials.

where $A$ stands for the cross-section area of the passage and $\Gamma$ represents the contour of the cross-section area, see Fig. 2. Therefore, once the solution of Eq. (7) is available, Eq. (10) provides temperature solution for any variation of boundary temperature, prescribed heat flux, initial condition, volumetric heat source, frictional heating, etc. A numerical study of all possible cases can become voluminous; however, flow though a porous medium bounded between two parallel plates is included mainly to illustrate the procedure.

There are three contributions on the right side of Eq. (10). The first term represents the contribution of the boundary condition, the second term includes the effect of frictional heating, and the last term describes the effects of the temperature field at the entrance location. Accordingly, the remaining portion of this presentation discusses the study of the effect of these three contributions to flow in parallel plate channels.

### 4.1. General effects of frictional heating

The Brinkman momentum equation includes addition of the Darcy term $\mu\mathbf{V}/K$ to the classical momentum equation while the $\mu\nabla^2\mathbf{V}$ term is replaced with $\mu_e\nabla^2\mathbf{V}$; the vector $\mathbf{V}$ is the local velocity vector. Accordingly, after replacing the fluid viscosity $\mu$ with the effective viscosity $\mu_e$ [1] and assuming local thermal equilibrium, the classical relation between the stress tensor and the deformation tensor provides the Brinkman momentum equation. In the Brinkman momentum equation, the term $\mu\mathbf{V}/K$ behaves as internal force per unit volume acting on a volume element and its contribution to the energy equation is $(\mu\mathbf{V}/K)\cdot\mathbf{V}$. Also, for flow in ducts, the contribution of frictional heating near the wall should be included. Three different models are presented and used in Nield et al. [7] to analyze the effect of frictional heating for parallel plate channels. The first model ignores the frictional heating at the wall and, in this case, the source term to become $S = \mu u^2/K$. The source term in the second model is $S = \mu u^2/K - \mu_e u\nabla^2 u$ for a parallel plate channel [7]. In the third model, the source term is $S = \mu u^2/K + \mu(\partial u/\partial y)^2$ for parallel plate channels [7]. The basic theories for the first two cases are discussed in [9]. Al-Hadhrame et al. [10] discusses theories presented in [9] and introduces a new model that was used in the third model [7] with a modification; that is, replacing the effective viscosity with the fluid viscosity to account for the contribution of frictional heating at the wall. To verify the suitability of the frictional heating in the third model [7], independent derivations were carried out. During formulation, the stress tensor, a deformation tensor, and a relation between these two tensors that produces the Brinkman momentum equation were utilized. Using the classical approach, this formulation yields the energy equation that agrees with the theoretical model in Al-Hadhrami et al. [10] not that in [7]. Therefore, in this study, the following quantity defines the contribution of the volumetric heat source

$$S = \mu u^2/K + \mu_e\Phi = \mu u^2/K + \mu_e[(\partial u/\partial y)^2 + (\partial u/\partial z)^2] \tag{11}$$

for fully-developed flow through a passage filled with fully saturated porous materials.

### 4.2. Temperature solution

In accordance with Eq. (12) and for the convenience of this presentation, the dimensionless temperature, for the passage shown in Fig. 2, is decomposed into two contributions,

$$\frac{T - T_1}{T_2 - T_1} = \Theta_S(y,z;x) + \Theta_W(y,z;x) \tag{12}$$

where $\Theta_S(y,z;x)$ presents the contribution of frictional heating and $\Theta_W(y,z;x)$ describes the effect of temperature change at the wall. When $x \leqslant x_o$, there is no temperature change at the wall $\Theta_W(y,z;x) = 0$, and $\Theta_S(y,z;x)$ is the temperature solution. This solution extends to other values of $x > x_o$. The Green's solution for $\Theta_S(y,z;x)$, using the conditions $\Theta_S(y,z;0) = 0$ and $\Theta_S(y,z;x)|_{wall} = 0$, is

$$\Theta_S(y,z;x) = \frac{1}{C(T_2 - T_1)} \times \int_{\xi=0}^{x} d\xi \int_A G(y,z;\xi|y',z';\xi) S(y',z';\xi)\, dA' \tag{13a}$$

Since the function $\Theta_W(y,z;x)$ has a zero value when $x, x_o$, this serves as the condition at $x - x_o$. The wall condition when $x > x_o$ is $\Theta_W(y,z;x)|_{wall} = 1$. The solution for $\Theta_W(y,z;x)$ is readily available in the literature [11] for different porous passages in the form of

$$\Theta_W(y,z;x - x_o) = 1 - \Theta_I(y,z;x - x_o) \tag{13b}$$

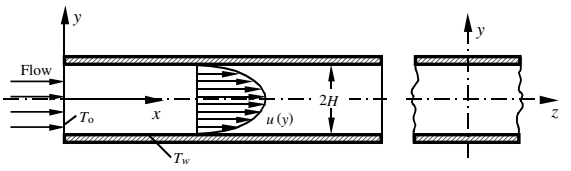


Fig. 3. A schematic a parallel plate channel.

where

$$\Theta_I(y,z;x-x_o)=\int_A uG(y,z;x-x_o|y',z';0)\,dA' \tag{13c}$$

Following substitution in Eq. (12), one obtains

$$\frac{T-T_1}{T_2-T_1}=\Theta_S(y,z;x)+1-\Theta_I(y,z;x) \tag{14a}$$

that becomes

$$\begin{aligned}\frac{T-T_2}{T_1-T_2}&=\Theta_I(y,z;x)-\Theta_S(y,z;x)\\&=\int_A uG(y,z;x-x_o|y',z';0)\,dA'+\frac{1}{C(T_1-T_2)}\\&\quad\times\int_{\xi=0}^{x}d\xi\int_A G(y,z;\xi|y',z';\xi)S(y',z';\xi)\,dA'\end{aligned} \tag{14b}$$

and it is used in subsequent computations. The change of $(T_2-T_1)$ to $(T_1-T_2)$ in the second term of Eq. (14b) is responsible for the sign change.

Because the exact nature of analysis is based on the Green's function solution, it is necessary to define the Green's function for a specific passage. A selected duct configuration is a parallel plate channel in Fig. 3. The frictional heating begins at $x=0$ assuming a constant temperature field $T_o=T_1$ at $x=0$ and $T_w=T_1$ when $x<x_o$, see Fig. 2. At $x=x_o$, there is a wall temperature jump and $T_w=T_2$ when $x>x_o$. Fig. 3 also depicts the coordinate systems and boundary conditions for this passage.

## 5. Frictional heating in parallel plate channels

Primarily, it is necessary to compute the Green's function. As an illustration, for flow between two parallel plates, a dimensionless distance $2H$ apart, Haji-Sheikh and Vafai [11] presented a solution in the absence of frictional heating and axial conduction that can be written using dimensionless parameters as

$$\Theta_I(\bar{y},\bar{x})=\frac{1}{N_m}\int_0^1\sum_{m=1}^{\infty}\left[\frac{u(\bar{y}')}{U}\right]Y_m(\bar{y})Y_m(\bar{y}')\,e^{-\lambda_m^2\bar{x}}\,d\bar{y}' \tag{15a}$$

where $\bar{y}=y/H$ and $\vec{x}=(x-x_o)/(HPe)$ following a transformation of $x$-axis. The orthogonality condition leads to the relation

$$\int_0^1\left(\frac{u}{U}\right)Y_m(\bar{y})Y_n(\bar{y})\,d\bar{y}=\begin{cases}0 & \text{when } n\neq m\\ N_m & \text{when } n=m\end{cases} \tag{15b}$$

wherein the norm is

$$\begin{aligned}N_m&=\int_0^1\left(\frac{u}{U}\right)[Y_m(\bar{y})]^2\,d\bar{y}\\&=\frac{1}{2\lambda_m}\left[\frac{\partial Y_m(\bar{y})}{\partial\bar{y}}\right]_{\bar{y}=1}\times\left[\frac{\partial Y_m(\bar{y})}{\partial\lambda_m}\right]_{\bar{y}=1}\end{aligned} \tag{15c}$$

The boundary conditions are $\Theta=0$ at the walls, when $y=\pm H$. Comparing Eq. (14) with Eq. (15a) suggests

$$G(\bar{y},\bar{x}|\bar{y}',0)=\frac{1}{N_m}\sum_{m=1}^{\infty}Y_m(\bar{y})Y_m(\bar{y}')\,e^{-\lambda_m^2\bar{x}} \tag{16a}$$

then

$$G(\bar{y},\bar{x}|\bar{y}',\xi)=\frac{1}{N_m}\sum_{m=1}^{\infty}Y_m(\bar{y})Y_m(\bar{y}')\,e^{-\lambda_m^2(\bar{x}-\xi)} \tag{16b}$$

and the description of function $Y_m(\bar{y})$ is to follow. The Green's function, as given by Eq. (16b), can be exported and placed within the generalized formulation of the Green's function solution in order to obtain the contribution of frictional heating and other possible variable wall temperature conditions. Further modifications are needed in order to predict the effects of axial conduction and/or the fin effect. Accordingly, for flow between two parallel plates, the function $Y_m(\bar{y})$ [11] can serve to find the temperature increase due to frictional heating. For flow between two parallel plates, the solution of the Brinkman momentum equation yields the fully developed velocity profile

$$\frac{u}{U}=\frac{\bar{u}}{\overline{U}}=\frac{\omega}{\omega-\tanh(\omega)}\left[1-\frac{\cosh(\omega\bar{y})}{\cosh(\omega)}\right] \tag{17}$$

where $\omega=(MDa)^{-1/2}$ is related to the Darcy number $Da=K/H^2$ and viscosity ratio $M=\mu_e/\mu$. Using a series solution, the following relations yield the function $Y_m(\bar{y})$,

$$Y(\bar{y})=\sum_{n=0}^{\infty}c_n(\bar{y})^{2n} \tag{18}$$

Fig. 3(a) indicates there is symmetry about $\bar{y}=y/H=0$ since the plates are $2H$ apart. The constants $c_n$ are obtainable from the recursive relation [11]

$$c_0=1 \quad \text{and}$$

$$c_n=-\frac{\omega^2\psi(c_{n-1}-d_{n-1})}{4n^2-2n} \quad \text{for } n\geqslant 1 \tag{19a}$$

where

$$\psi=\frac{\lambda^2/\omega}{\omega-\tanh(\omega)} \tag{19b}$$

contains the eigenvalues $\lambda = \lambda_m$ to be determined numerically. The other parameter in Eq. (19a) is

$$d_n = \sum_{j=0}^{n} c_j \frac{1/\cosh(\omega)}{[2(n-i)]!}(\omega)^{2(n-j)} \tag{19c}$$

Based on Eq. (12) with Green's function taken from Eq. (16b), the temperature solution that includes the contribution of frictional heating is

$$\begin{aligned}\frac{T(\bar{y},\bar{x})-T_2}{T_1-T_2} &= \int_0^1 \sum_{m=1}^{\infty} \frac{1}{N_m}\left[\frac{u(\bar{y}')}{U}\right] Y_m(\bar{y}) Y_m(\bar{y}') \Theta_{\mathrm{I}}(\bar{y}',0)\, \mathrm{e}^{-\lambda_m^2 \bar{x}}\, \mathrm{d}\bar{y}' \\ &+ \frac{Ec\,Pr}{M\,Da} \int_0^1 \sum_{m=1}^{\infty} \left(\frac{1}{N_m}\right)\left\{\left[\frac{u(\bar{y}')}{U}\right]^2 \right. \\ &\left. + M\,Da\left[\frac{\partial}{\partial \bar{y}'}\left(\frac{u(\bar{y}')}{U}\right)\right]^2\right\} Y_m(\bar{y}) Y_m(\bar{y}') \\ &\times \frac{1-\mathrm{e}^{-\lambda_m^2(\bar{x}+\bar{x}_{\mathrm{o}})}}{\lambda_m^2}\mathrm{d}\bar{y}' \end{aligned} \tag{20}$$

where $Da = K/H^2$ is the Darcy number, $Ec = U^2/[c_p(T_1 - T_2)]$ is the Eckert number, $Pr = \mu_{\mathrm{e}} c_p/k_{\mathrm{e}}$ is the Prandtl number, $M = \mu_{\mathrm{e}}/\mu$, and $\bar{x}_{\mathrm{o}} = x_{\mathrm{o}}/(H\,Pe)$. The Brinkman number, $Br$, commonly defined in the porous media literature, is $Br = (Ec\,Pr)/(M\,Da)$ or $Br = \mu U^2 H^2/[K k_{\mathrm{e}}(T_1 - T_2)]$. Therefore, according to this definition, the value of $Br$ can become negative if $T_2 > T_1$. When $\Theta_{\mathrm{I}}(\bar{r}', 0) = 1$, the first integral on the right side of Eq. (20) becomes

$$\int_0^1 \left[\frac{u(\bar{y}')}{U}\right] Y_m(\bar{y}')\,\mathrm{d}\bar{y}' = -\frac{1}{\lambda_m^2}\left[\frac{\mathrm{d}Y_m(\bar{y}')}{\mathrm{d}\bar{r}'}\right]_{\bar{r}'=1}$$

Once the temperature field is determined from Eq. (20), the heat transfer coefficient is obtainable from the definition that $q_{\mathrm{w}} = h(T_{\mathrm{w}} - T_{\mathrm{b}})$ where

$$T_{\mathrm{b}} = \frac{1}{A}\int_A \left(\frac{u}{U}\right) T\,\mathrm{d}A \tag{21}$$

In the absence of frictional heating, the functional behavior of the first term in Eq. (20) is well documented in [11] and eigenvalues are presented for selected $M\,Da$ values. The convergence of the first term in Eq. (20) depends on the value of $\exp(-\lambda_m^2 \bar{x})$. As an example, when $M\,Da = 0.1$, the 10th eigenvalue is $\lambda_{10}^2 = 922.9$. Therefore, it is possible to have a solution with, e.g., 5 digit accuracy when $\lambda_m^2 \bar{x} > 11.5$, that is, $\bar{x} > 0.012$. Moreover, a solution having 35 eigenvalues, with $\lambda_{35}^2 = 12325.7$, yields results with similar accuracy when $\bar{x} > 0.0009$.

The contribution of the frictional heating in Eq. (20), in the absence of a wall temperature change, is

$$\begin{aligned}\frac{k_{\mathrm{e}}[T(\bar{y},\bar{x})-T_1]}{\mu_{\mathrm{e}}U^2} &= \frac{\Theta_{\mathrm{S}}(\bar{y},\bar{x})}{Pr\,Ec} \\ &= \frac{1}{M\,Da}\int_0^1 \sum_{m=1}^{\infty}\left(\frac{1}{N_m}\right)\left\{\left[\frac{u(\bar{y}')}{U}\right]^2 \right. \\ &\left. + M\,Da\left[\frac{\partial}{\partial \bar{y}'}\left(\frac{u(\bar{y}')}{U}\right)\right]^2\right\} Y_m(\bar{y}) Y_m(\bar{y}') \\ &\times \frac{1-\mathrm{e}^{-\lambda_m^2(\bar{x}+\bar{x}_{\mathrm{o}})}}{\lambda_m^2}\mathrm{d}\bar{y}' \end{aligned} \tag{22}$$

The corresponding wall heat flux, using $q_{\mathrm{w}} = -k_{\mathrm{e}}\partial T/\partial y$ at $y = H$, leads to the relation

$$\begin{aligned}\frac{Hq_{\mathrm{w}}(\bar{x})}{\mu_{\mathrm{e}}U^2} &= -\frac{1}{M\,Da}\int_0^1 \sum_{m=1}^{\infty}\left(\frac{1}{N_m}\right)\left\{\left[\frac{u(\bar{y}')}{U}\right]^2 \right. \\ &\left. + M\,Da\left[\frac{\partial}{\partial \bar{y}'}\left(\frac{u(\bar{y}')}{U}\right)\right]^2\right\} \\ &\times \left[\frac{Y_m(\bar{y})}{\mathrm{d}\bar{y}}\right]_{\bar{y}=1} Y_m(\bar{y}')\frac{1-\mathrm{e}^{-\lambda_m^2(\bar{x}+\bar{x}_{\mathrm{o}})}}{\lambda_m^2}\mathrm{d}\bar{y}' \end{aligned} \tag{23}$$

This heat flux relation has several advantages. The right side of equation depends on $\bar{x} + \bar{x}_{\mathrm{o}} = x/(H\,Pe)$ and $M\,Da$ serves as the only parameter. The convergence of Eq. (23) in its present form is poor. The remedial steps to improve its convergence are to appear later. The value of the dimensionless heat flux for different $M\,Da$ is plotted as a function $x/(H\,Pe)$ in Fig. 4(a). For a large range of the axial coordinate, the heat flux data, when $M\,Da$ is small, are in a reasonably good agreement with an asymptotic solution when $u/U = 1$. The asymptotic relation is obtained using standard Fourier series solution (when $u = U$); that is

$$\left.\frac{Hq_{\mathrm{w}}(\bar{x})}{\mu_{\mathrm{e}}U^2}\right|_{M\,Da\to 0} = -\frac{2}{\pi^2 M\,Da}\sum_{m=0}^{\infty}\frac{1-\exp[(m-1/2)^2\pi^2 x/(H\,Pe)]}{(m-1/2)^2}$$

This indicates that the wall influence on the frictional heating is small when $M\,Da$ is small. Also, Fig. 4(b) shows the average wall heat flux $Hq_{\mathrm{w,ave}}(\bar{x})/(\mu U^2)$ obtained using the relation

$$\bar{q}_{\mathrm{w}} = \frac{1}{x}\int_0^x q_{\mathrm{w}}\,\mathrm{d}x \tag{24}$$

The asymptotic behavior of $\bar{q}_{\mathrm{w}}$ is also included in Fig. 4(b). Once $q_{\mathrm{w}}$ and $\bar{q}_{\mathrm{w}}$ are known, all other information such as local/average heat transfer coefficients and bulk temperature are readily available.

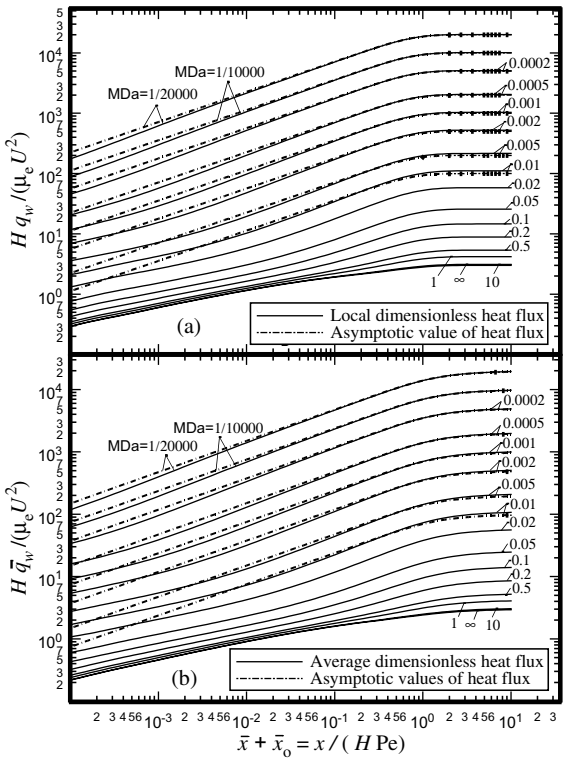


Fig. 4. The contribution of frictional losses to (a) local and (b) average heat flux for parallel plate channels.

The general formulation of the local heat transfer coefficient, at any location $\bar{x}$, is related to the bulk temperature through the relation

$$Nu = \frac{hL_c}{k_e} = -\left[\frac{d\Theta_b(\bar{x})/d\bar{x}}{\Theta_b(\bar{x})}\right] + \left[\frac{Br}{\Theta_b(\bar{x})}\right] \times \int_0^1 \left[\left(\frac{u(\bar{y})}{U}\right)^2 + MDa\left(\frac{\partial(u/U)}{\partial\bar{y}}\right)^2\right] d\bar{y} \quad (25a)$$

where

$$\Theta_b(\bar{x}) = \int_0^1 \left(\frac{u}{U}\right)\Theta(\bar{y},\bar{x})\,d\bar{y} \quad (25b)$$

For this case, $L_c = H$, then $Pe = \rho c_p HU/k_e$ and $\bar{x} = (x - x_o)/(PeH)$. The value of dimensionless velocity $u/U$, Eq. (17), for inclusion in Eqs. (25a) and (25b), is

$$\frac{u}{U} = \frac{\omega[\cosh(\omega) - \cosh(\omega\bar{y})]}{\omega\cosh(\omega) - \sinh(\omega)} \quad (26)$$

wherein $\omega = (MDa)^{-1/2}$. The integral in Eq. (25a) has a fixed value for a given $MDa$ parameter, it is

$$\frac{1}{MDa}\int_0^1 \left[\left(\frac{u(\bar{y})}{U}\right)^2 + MDa\left(\frac{\partial(u/U)}{\partial\bar{y}}\right)^2\right] d\bar{y} = \frac{\omega^3}{\omega - \tanh(\omega)} \quad (27)$$

In addition to the dimensionless axial coordinate, the local and average Nusselt numbers depend on $MDa$ and $Br$. Therefore, it is simpler to present the local and average heat flux in a single graph and, if needed, one can combine the result with the wall heat flux due to a change in the wall temperature. Using the value of heat flux from Eq. (23), the bulk temperature is obtainable by using Eq. (27) in application of the first law of thermodynamics to a material element as

$$\frac{k_e[T_b(\bar{x}) - T_1]}{\mu_e U^2} = \left[\frac{\omega^3}{\omega - \tanh(\omega)} - \frac{H\bar{q}_w}{\mu_e U^2}\right](\bar{x} + \bar{x}_o) \quad (28)$$

and subsequently, the local Nusselt number is

$$Nu_H = \frac{Hh}{k_e} = \frac{Hq_w/(\mu_e U^2)}{\left[\frac{\omega^3}{\omega - \tanh(\omega)} - \frac{H\bar{q}_w}{\mu_e U^2}\right](\bar{x} + \bar{x}_o)} \quad (29)$$

The term in square brackets in Eq. (28) approaches 0 as $\bar{x} \to \infty$; however the left side of Eq. (28) assumes a fixed value for any given $MDa$; the following relation provides the limiting values as $\bar{x} \to \infty$,

$$\left.\frac{k_e[T_b(\bar{x}) - T_1]}{\mu_e U^2}\right|_{\bar{x}\to\infty} = F_S(\omega) = \frac{\omega^2}{48}\left[\frac{1}{\omega\cosh(\omega) - \sinh(\omega)}\right]^3 \times \left[(12\omega^3 - 150\omega)\cosh(\omega) + (4\omega^3 - 30\omega)\cosh(3\omega) + 57\sinh(\omega) + 41\sinh(3\omega)\right] \quad (30a)$$

where $F_S(\omega)$ is a source function. An approximate form of this source function, Eq. (30a), with an error of less than 2% for $10^{-5} < MDa < 50$, is

$$F_S(MDa) \cong \frac{1}{3MDa} + \left[\frac{0.62 + 0.465(MDa)^{-1}}{1 + 0.2(MDa)^{-1/5}}\right]^{2/3} \quad (30b)$$

The first term in Eq. (30b) describes the limit as $MDa$ becomes small and approaches $1/(3MDa)$ while the limit, as $MDa$ becomes large and goes to infinity, is 24/35. Fig. 5 compares the exact and approximate values for the limiting values of the bulk temperature.

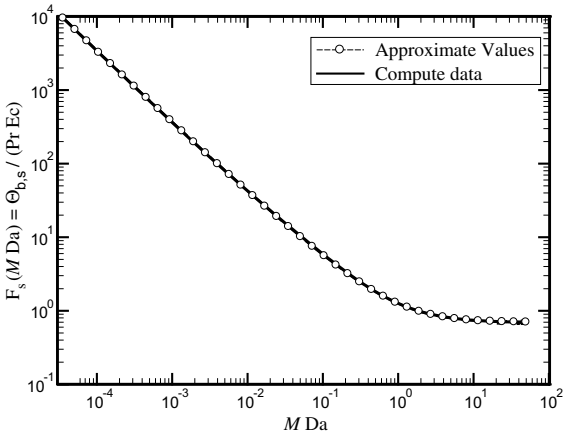


Fig. 5. The asymptotic behavior of the bulk temperature in Eq. (30a) and approximate values, Eq. (30b).

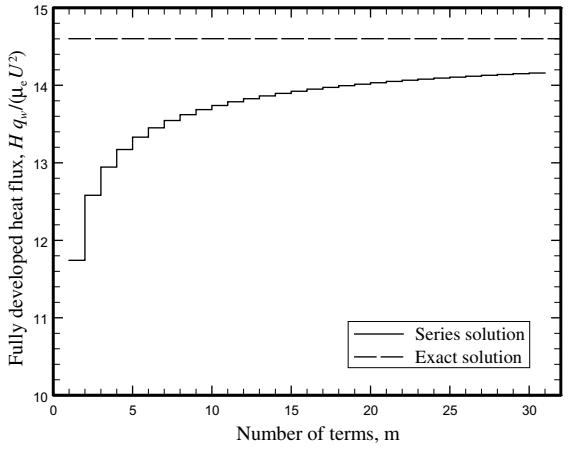


Fig. 6. The convergence of heat flux solution for parallel plate channels as the number of terms $m$ increases.

Therefore, when $x_o$ is sufficiently large, this relation provides the bulk temperature at the entrance of the heated section.

The convergence of Eq. (22) is, at best, slow and the convergence of Eq. (23) is not satisfactory. As an illustration, using $MDa = 0.1$, the data in Fig. 6 show, at large values of $\bar{x}$, there is a large deviation between a solution based on Eq. (23) and its exact limiting value, Eq. (27). An examination of Eq. (20) shows that the solution has two contributions: a fully developed solution and a complementary entrance solution,

$$\Theta_S(\bar{y},\bar{x}) = \Theta_{S,fd}(\bar{y},\bar{x}) - \Theta_{S,ce}(\bar{y},\bar{x}) \tag{31a}$$

where

$$\Theta_{S,fd}(\bar{y},\bar{x}) = \frac{Pr\,Ec}{M\,Da}\int_0^1 \sum_{m=1}^{\infty}\left(\frac{1}{N_m}\right)\left\{\left[\frac{u(\bar{y}')}{U}\right]^2 + M\,Da\left[\frac{\partial}{\partial\bar{y}'}\left(\frac{u(\bar{y}')}{U}\right)\right]^2\right\}\frac{Y_m(\bar{y})Y_m(\bar{y}')}{\lambda_m^2}\,d\bar{y}' \tag{31b}$$

and

$$\Theta_{S,ce}(\bar{y},\bar{x}) = \frac{Pr\,Ec}{M\,Da}\int_0^1 \sum_{m=1}^{\infty}\left(\frac{1}{N_m}\right)\left\{\left[\frac{u(\bar{y}')}{U}\right]^2 + M\,Da\left[\frac{\partial}{\partial\bar{y}'}\left(\frac{u(\bar{y}')}{U}\right)\right]^2\right\} \times \frac{Y_m(\bar{y})Y_m(\bar{y}')}{\lambda_m^2}e^{-\lambda_m^2(\bar{x}+\bar{x}_o)}\,d\bar{y}' \tag{31c}$$

The complementary entrance solution has an excellent convergence characteristic. For example, when $MDa = 0.1$, the 10th eigenvalue is $\lambda_{10}^2 = 922.9$ and one can obtain data at $\bar{x} = 0.005$ with an error of the order of $10^{-5}$ by employing 10 eigenvalues. In order to improve the accuracy of $\Theta_S(\bar{y},\bar{x})$, the fully developed component $\Theta_{S,ss}(\bar{y},\bar{x})$ should be replaced by the exact fully developed solution, that is,

$$\Theta_{S,fd}(\bar{y},\bar{x}) = \frac{\omega^2}{4[\omega-\tanh(\omega)]^2}\Big\{2\omega^2(1-\bar{y}^2) - 8[1-\cosh(\omega\bar{y})/\cosh(\omega)] + [\cosh(2\omega)-\cosh(2\omega\bar{y})]/\cosh^2(\omega)\Big\} \tag{32}$$

The heat flux, Eq. (23), also has two solutions: a fully developed and a complementary entrance. The fully developed solution component of Eq. (23), as appeared earlier, is on the right side of Eq. (27). A similar procedure was used to improve convergence of transient conduction problems in [12]. Therefore, for a better accuracy, Eq. (23) takes the following form

$$\frac{Hq_w(\bar{x})}{\mu_e U^2} = \frac{\omega^3}{\omega-\tanh(\omega)} + \frac{1}{M\,Da}\int_0^1 \sum_{m=1}^{\infty}\left(\frac{1}{N_m}\right) \times \left\{\left[\frac{u(\bar{y}')}{U}\right]^2 + M\,Da\left[\frac{\partial}{\partial\bar{y}'}\left(\frac{u(\bar{y}')}{U}\right)\right]^2\right\} \times \left[\frac{Y_m(\bar{y})}{d\bar{y}}\right]_{\bar{y}=1} Y_m(\bar{y}')\frac{e^{-\lambda_m^2(\bar{x}+\bar{x}_o)}}{\lambda_m^2}d\bar{y}' \tag{33}$$

The complementary entrance solution converges slightly slower than that for Eq. (31c) due to the derivative at $\bar{y} = 1$. When using Eq. (21) to compute the bulk temperature, there will be a bulk temperature component due to the fully developed solution and one due to the complementary entrance solution. Integration over the area enhances the convergence of the complementary entrance solution. The exact solution for the bulk temperature component is $F_S(\omega)$ in Eq. (30).

*Numerical example*. The objective is to demonstrate the combined effects of the contribution of frictional heating and wall temperature change to the overall values of the Nusselt number $hH/k$, Eq. (25a). All computations are performed symbolically on Mathematica [13]. This example discusses solutions for two limiting cases. When $x_o$ is sufficiently large, the right side of Eq. (30a) describes the contribution of frictional heating to the bulk temperature. Eqs. (20) and (25) include the contribution of wall temperature change to the bulk temperature and viscous dissipation; they are computed in addition to the surface heat flux. This information provides the overall heat transfer coefficient plotted in Fig. 7(a) for $M\,Da = 1$. The value of $M\,Da = 1$ is selected mainly to compare the results with those in [7]. The data designated by "±" symbols were graphically scanned from Ref. [7, Fig. 10b] and they correspond to a large Peclet number. There is a remarkably good agreement between the scanned data and the present data.

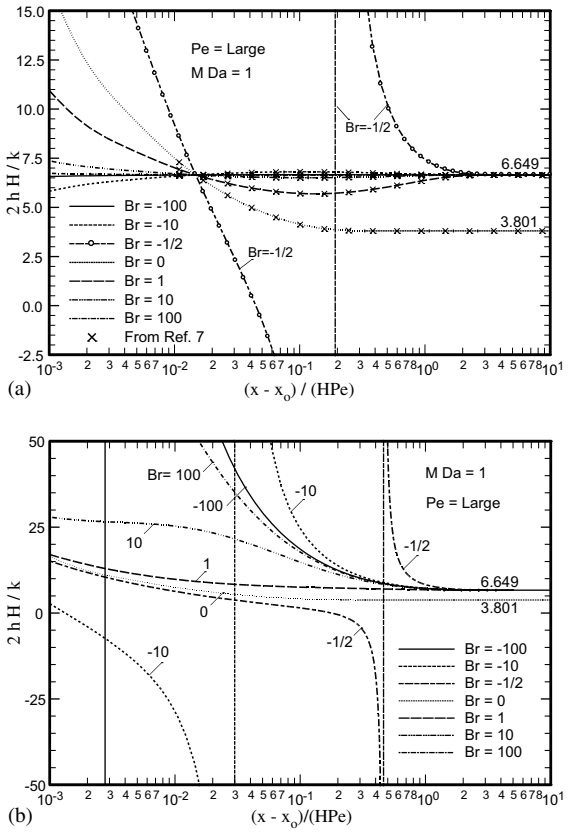


Fig. 7. Heat transfer coefficient for fully developed flow in parallel plate channels when, (a) for large $x_o$ and (b) $x_o = 0$.

According to Eq. (28), for large Pe and $M\,Da = 1$, one would expect singularities to appear when $0 > Br > -0.792$. Therefore, an additional set of data for $Br = -1/2$ is included and the range of data is extended in order to show the existence of singularities. This is to demonstrate, when $Br$ is less than 0, it is possible for the heat transfer coefficient to become infinite depending on the parameters $\bar{x}_o$, $Da$ and $Br$. As a demonstration of this concept, the data in Fig. 7(a) are reproduced when $Br$ is negative and $x_o = 0$; the data are plotted in Fig. 7(b). This figure clearly shows the appearance of singularities for $Br = 1/2$, 10, and 100.

## 6. Discussion

The numerical example shows the utility of the Green's function solution method. Also, it demonstrates the overall contribution of the frictional heating in channel flow including that for the wall heat flux. The effect of wall temperature change on the wall heat flux is deterministic in a similar manner as shown in [11] and correlations for local and average heat transfer coefficients are in [14]. Each of these contributions can provide a corresponding heat transfer coefficient. In fact, the knowledge of average heat transfer coefficient is of great significance as it allows practitioners to easily compute the bulk temperature from a classical relation

$$\frac{T_{b,I} - T_2}{T_1 - T_2} = \exp\left[-\frac{\bar{h}Cx}{\rho UAc_p}\right] = \exp[-\overline{N}u_H\bar{x}] \tag{34}$$

Once $T_{b,I}$ is known, then the local heat flux and the average heat flux, due to the effect of wall temperature change, is readily available: $q_{w,I} = h(T_2 - T_{b,I})$ and $\bar{q}_{w,I} = \rho UAc_p(T_2 - T_{b,I})/(C\bar{x})$. Note that, in this presentation, $q_w$ is the heat flux due to frictional heating and it is positive leaving the system; this must be considered when evaluating $q_{w,S}$.

Accordingly, one can use the available knowledge of heat transfer coefficient in the absence of frictional heating to compute the effect of wall temperature change. Also, this study discusses the sole effect of frictional heating to begin from any location depending on the value of $x_o$. The methodology presented is applicable to laminar MHD flow through a parallel-plate channel [15] after some modifications that include an additional heat source term. These combined effects provide a desirable flexibility and will simplify the presentation of data as it reduces the needed parameters for each case. A

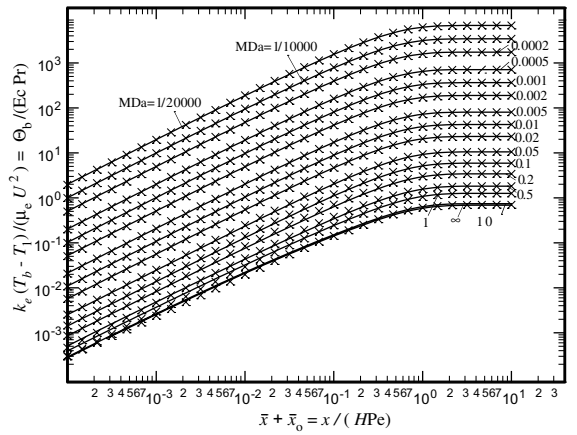


Fig. 8. The bulk temperature in parallel plates channels for different $M\,Da$ values. The discrete data are from correlations in Eqs. (40) and (43).

proper combination of these two contributions yields the value of bulk temperature

$$T_b - T_1 = (T_{b,S} - T_1) + (T_{b,I} - T_1) \tag{35}$$

To facilitate the evaluation of $T_b$, the contribution of frictional heating, $T_{b,S}$ is plotted in Fig. 8 for parallel plate channels. Also, the combined effect of frictional heating and wall temperature change to the local wall heat flux is

$$q_w = q_{w,S} + q_{w,I} \tag{36}$$

and to the average wall heat flux is

$$\bar{q}_w = \bar{q}_{w,S} + \bar{q}_{w,I} \tag{37}$$

The computation of the bulk temperature from the local heat transfer coefficient for the combined effects, emphasized in the literature, would require extensive numerical simulations. The data presented here, combined with those in [14], can simplify the evaluation of heat transfer in these passages.

Finally, it is possible to provide simple correlations for rapid estimation of the dimensionless wall heat flux. For local wall heat flux, the following correlation yields reasonably small error ±5% when $M\,Da$ is small,

$$\frac{Hq_w}{\mu_e U^2} \cong \left[\frac{\omega^3}{\omega - \tanh(\omega)}\right]\left\{1 - \left[\frac{1 - c_1(\bar{x} + \bar{x}_o)^{c_2}}{[1 + c_3(\bar{x} + \bar{x}_o)]^{1.75}}\right]\right\} \tag{38}$$

with

$$c_1 = 0.8 - 0.5[1/(0.00045\omega^2 + 0.75)]^2 + 0.9\omega^{-2/3},$$
$$c_2 = 0.5 - 0.28[1/(0.001\omega^2 + 1)]^2,$$
$$c_3 = 1.1 + 0.4[\omega^{-2}/(1 + \omega^{-2})]^{2.5}$$

The correlation for the average wall heat flux has a similar form that contains fully developed term and the complementary transient term,

$$\frac{H\bar{q}_w}{\mu_e U^2} \cong \left[\frac{\omega^3}{\omega - \tanh(\omega)}\right]\left\{1 - \left[\frac{1 - c_1(\bar{x} + \bar{x}_o)^{c_2}}{1 + c_3(\bar{x} + \bar{x}_o)}\right]\right\} \tag{39}$$

As before, the parameters $c_1$, $c_2$, and $c_3$ depend on the value of $M\,Da$ using the relations

$$c_1 = 0.7 - 0.4/[1 + 2.5\omega^{-5/2}],$$
$$c_2 = 0.195 + 0.174/[1 + 10\omega^{-2}],$$
$$c_3 = 0.85 + (0.5 - \omega^{-1/2})/(1 + \omega^{-2})$$

These equations provide reasonable accuracies, with error of ±5%, when $M\,Da$ is small. The error becomes larger when $M\,Da$ approaches 0.2. Theoretically, it is possible to use the correlation for the dimensionless average wall heat flux and Eq. (28) in order to obtain the dimensionless bulk temperature; however, the error may become unreasonably large. Therefore, the following direct correlation of the bulk temperature yields a better accuracy,

$$\frac{k_e[T_b(\bar{x}) - T_1]}{\mu_e U^2} \cong \frac{F_S(\omega)}{1 + F_S(\omega)\dfrac{[c_1 + c_2/(\bar{x} + \bar{x}_o)]^{c_3}}{1 + 5.63(\bar{x} + \bar{x}_o)^{11/4}}} \tag{40}$$

where $c_1 = 0.34/(1.45 + \omega^3)$, $c_2 = \omega^{-2}/(1 + 1.3\omega^{-1.6})^{5/4}$, $c_3 = 1 - 0.07/(1 + \omega^4)$ and Eq. (30) provides the value of $F_S(\omega)$. The "±" symbols in Fig. 8 are computed using Eq. (40). In general, the symbols agree well with the analytical results shown as the solid lines. Their error is within the targeted accuracy of ±5% when $M\,Da$ is relatively small. The error becomes larger when $M\,Da$ is much larger than 10 and, in that range, the error approaches 10%.

When $M\,Da$ is larger than 1, one can modify and use the correlations for frictional heating in unobstructed channels. For an unobstructed channel, the following relations can provide: the local wall heat flux, with an error of less than 5%,

$$\frac{Hq_w}{\mu_e U^2} \cong \frac{3 + 5.47/(\bar{x} + \bar{x}_o) - 0.134/(\bar{x} + \bar{x}_o)^{1.25}}{[1 + 1.4/(\bar{x} + \bar{x}_o)]^{1.24}} \tag{41}$$

the average wall heat flux, with an error of less than 2.5%,

$$\frac{H\bar{q}_w}{\mu_e U^2} \cong \frac{3 + 2.2/(\bar{x} + \bar{x}_o)^{1.08} - 0.05/(\bar{x} + \bar{x}_o)^{1.34}}{(1 + 0.76/(\bar{x} + \bar{x}_o))^{1.34}} \tag{42}$$

and the bulk temperature, with an error of less than 4%,

$$\frac{k_e[T_b(\bar{x}) - T_1]}{\mu_e U^2} \cong \frac{0.6857\tanh[1.265(\bar{x} + \bar{x}_o)^{0.78}]}{\left[1 + 0.02(\bar{x} + \bar{x}_o)^{-0.6}\right]^{0.5}} \tag{43}$$

In these relations, the fully developed conditions as $(\bar{x} + \bar{x}_o) \to \infty$ is 3 in Eqs. (41) and (42) and it is 0.6857 in Eq. (43). Therefore, when $M\,Da$ is larger than 1, as an

approximation, one can replace 3 in Eqs. (41) and (42) with the corresponding quantity from Eq. (27) and replace 0.6857 in Eq. (43) with the value of $F_S(\omega)$ from (30b).

## 7. Conclusion

The Green's function solution method is a powerful tool for solving heat transfer problems for flow through ducts. With the Green's function available, one can compute various effects, e.g., frictional heating, wall temperature change, entrance thermal conditions, and fin effect. Furthermore, the Green's function solution can be extended to include the effect axial conduction. Also, as a parallel application, the method of weighted residuals enhances this Green's function solution to accommodate the ducts with non-orthogonal flow passage profiles.

The data in Fig. 4 show that the thermal effect due to frictional heating at the duct walls becomes significant only when $MDa$ is relatively large. Therefore, the first model in Ref. [7] is adequate in a variety of applications. In general, the frictional heating has a significant contribution to the temperature field depending on the values of $MDa$ and $MDa$. When $MDa$ is relatively small, the dimensionless bulk temperature can have a significant value when $EcPr$ is also small. In contrast, for unobstructed channels, $MDa$ goes to infinity while, e.g., a value of $EcPr = 0.1$ can produce a measurable effect on the overall bulk temperature.

The study of flow condition suggests data to be presented for frictional heating alone for two reasons. Primarily, it reduces the number of needed parameters for an archival consideration of data. These results in conjunction with existing data in [11,14] can enhance the ability of the user to acquire information for the frictional effect in the presence of different unheated entrance lengths.

## References

[1] M. Kaviany, Laminar flow through a porous channel bounded by isothermal parallel plates, Int. J. Heat Mass Transfer 28 (4) (1985) 851–858.

[2] D.A. Nield, A. Bejan, Convection in Porous Media, second ed., Springer-Verlog, New York, 1999.

[3] K. Kaviany, Principles of Heat Transfer in Porous Media, Springer-Verlag, New York, 1991.

[4] K. Vafai (Ed.), Handbook of Porous Media, Marcel Dekker, New York, 2000.

[5] D. Angirasa, Forced convective heat transfer in metallic fibrous materials, ASME J. Heat Transfer 124 (4) (2002) 739–745.

[6] J.V. Beck, K.D. Cole, A. Haji-Sheikh, B. Litkouhi, Heat Conduction Using Green's Functions, Hemisphere Publ. Corp., Washington, DC, 1992.

[7] D.A. Nield, A.V. Kuznetsov, M. Xiong, Thermally developing forced convection in a porous medium: parallel plate channel with walls at uniform temperature, with axial conduction and viscous dissipation effects, Int. J. Heat Mass Transfer 46 (4) (2003) 643–651.

[8] A.V. Kuznetsov, M. Xiong, D.A. Nield, Thermally developing forced convection in a porous medium: circular ducts with walls at constant temperature, with longitudinal conduction and viscous dissipation effects, Transport Porous Media 53 (3) (2003) 331–345.

[9] D.A. Nield, Resolution of paradox involving viscous dissipation and nonlinear drag in a porous medium, Transport Porous Media 41 (1) (2000) 349–357.

[10] A.K. Al-Hadhrami, L. Elliot, D.B. Ingham, A new model for viscous dissipation in porous media across a range of permeability values, Transport Porous Media 53 (1) (2003) 117–122.

[11] A. Haji-Sheikh, K. Vafai, Analysis of flow and heat transfer in porous media imbedded inside various-shaped ducts, Int. J. Heat Mass Transfer 47 (8–9) (2004) 1889–1905.

[12] J.V. Beck, A. Haji-Sheikh, D. Amos, D. Yen, Verification solution for partial heating of rectangular solids, Int. J. Heat Mass Transfer, in press.

[13] S. Wolfram, The Mathematica Book, fourth ed., Cambridge University press, Cambridge, UK, 1999.

[14] A. Haji-Sheikh, Estimation of average and local heat transfer in parallel plates and circular ducts filled with porous materials, ASME J. Heat Transfer 126 (3) (2004) 400–409.

[15] J. Lahjomri, A. Oubarra, A. Alemany, Heat transfer by laminar Hartmann flow in thermal entrance region with a step change in wall temperature: the Graetz problem extended, Int. J. Heat Mass Transfer 45 (5) (2002) 1127–1148.